Supplementary Materials

Unstable genome and transcriptome dynamics during tumor metastasis contribute to therapeutic heterogeneity in colorectal cancers

Sung-Yup Cho, Jeesoo Chae, Deukchae Na, Wonyoung Kang, Ahra Lee, Seoyeon Min, Jinjoo Kang, Boram Choi, Jieun Lee, Chang Ohk Sung, Jeffrey H. Chuang, Charles Lee, Won-Suk Lee, Hansoo Park, and Jong-Il Kim

S.-Y. Cho and J. Chae contributed equally to this article.

C. Lee, W.-S. Lee, H. Park and J.-I. Kim are considered co-senior authors.

Correspondence and requests for materials should be addressed to W.-S.L. (email: lws@gilhospital.com), to H.P. (email: hspark27@gist.ac.kr) or to J.-I.K. (email: jongil@snu.ac.kr)

Supplementary Materials and Methods

DNA preparation, exome capture, library construction and sequencing

Genomic DNAs were extracted from patient blood using the Gentra Puregene Blood Kit (Qiagen) and the tumor DNA was obtained from patients and PDX tumors using the DNeasy Blood & Tissue Kit (Qiagen). The 250 ng of DNA was sonicated with Covaris S220 Focusedultrasonicators and 101 bp paired-end libraries were constructed with the SureSelect All Exon V5 kit (Agilent). Whole exome sequencing (WES) was performed on an Illumina HiSeq 2000 instrument.

RNA preparation, library construction and RNA sequencing

RNA extraction from non-tumor tissues, patients and PDX tumors was performed using TRIzol™ (Invitrogen). Samples with RNA integrity number (RIN) of greater than 5 were further processed. The 101 bp paired-end libraries were constructed with the TruSeq RNA Sample Prep Kit v2 (Illumina) using 1 μg of RNA. Whole transcriptome sequencing (WTS) was performed on an Illumina HiSeq 2000 instrument.

Droplet Digital PCR (ddPCR)

The extracted genomic DNA was restricted with EcoRI (New England Biolabs) enzyme for 1 hr at 37°C. The PCR mixture was assembled in 20 μL solution containing 1X ddPCR supermix (Bio-Rad), 1X probe and primer premix for determining wild-type and mutant genes (ERBB2 L755S; final concentration of 250 nM for probe and 900 nM for each primer; Applied Biosystems), and 10 ng of the restricted DNA. The reaction mixture and droplet generation oil (Bio-Rad) were loaded into the droplet generator (QX-200; Bio-Rad). The droplets were transferred to a 96-well PCR plate and PCR reaction was performed as follows: enzyme activation for 10 min at 95°C, 40 cycles of 94°C for 30 sec, 60°C for 1 min, and 98°C for 10

min, followed by enzyme deactivation for 10 min at 98°C and 4°C hold (performed with a ramp rate of 2°C/sec in all steps). The PCR plate was placed in a droplet reader (Bio-Rad). After the reading, the allele frequencies of mutant genes were analyzed by Quanta software (Bio-Rad) accompanied by the droplet reader.

Cell culture

HEK-293 cells were obtained from the Korean Cell Line Bank in 2014 and maintained in DMEM medium (Thermo Fisher Scientific) containing 10% fetal bovine serum (Thermo Fisher Scientific). The characteristics of cells were tested and authenticated by Korean Cell Line Bank, and cells in early passages were used for experiment to minimize genetic changes. Penicillin (100 U/ml; Thermo Fisher Scientific) and streptomycin sulfate (100 μg/ml; Thermo Fisher Scientific) were supplemented to all cell culture media. All cells were maintained in a humidified incubator with 5% CO_2 at 37°C.

Site-directed mutagenesis and transfection of DNA

For recombinant DNA, physical and biologic containment procedures were practiced, in accord with the National Institutes of Health Guidelines for Research Involving Recombinant DNA Molecules. The QuickChange site-directed mutagenesis kit (Stratagene) was used to make point mutations, and the resulting mutations were verified by Sanger sequencing. The primers used in constructing the point mutations were as follows (the underlined sequences indicate the mutated bases): *TP53* A159V, 5'- CCCGCGTCCGCGTCATGGCCATCTAC -3' and *TP53* R273C, 5'- GAACAGCTTTGAGGTGTGCGTTTGTGCCTGTCCTG -3'. Transfection experiments were performed using the Lipofectamine 2000 Transfection kit according to manufacturer's recommendations (Thermo Fisher Scientific). After 48 hr, cells were harvested for cell viability assays in the presence of the selected drug.

Cell viability assay

For the cell viability assays, about 5,000 cells were placed in 96-well plates, treated with indicated drugs for 72 h and cell viabilities estimated using the EzCytox WST assay kit according to the manufacturer's instructions (Daeil Lab).

Quantitative real-time PCR

Total RNA was purified using the RNeasy Plus Mini Kit according to manufacturer's instructions (Qiagen). One microgram of total RNA was transcribed into cDNA using the Maxime RT PreMix (Intron Biotechnology) for 1 hr at 45°C. Quantitative real-time PCR was performed using SYBR Green PCR Master Mix (Applied Biosystems). Glyceraldehyde 3-phosphate dehydrogenase (*GAPDH*) was used as internal control for normalization. The sequences of primers for vimentin were 5'- CCAAACTTTTCCTCCCTGAACC -3' and 5'- GTGATGCTGAGAAGTTTCGTTGA -3', and the sequences for *GAPDH* were 5'- CGCTCTCTGCTCCTCCTGTT -3' and 5'- CCATGGTGTCTGAGCGATGT -3'.

Western blot analysis

Cells were lysed in RIPA buffer (Thermo Fisher Scientific), and then centrifuged at 20,000 g for 10 min at 4°C. After determination of protein concentration in the cell extract by the bicinchoninic acid assay (Thermo Scientific), 20 μg of protein were resolved by SDS-PAGE and transferred to a polyvinyl difluoride membrane. Membranes were blocked for 1 hr with 5% skim milk in Tris-buffered saline and then incubated with an anti-Myc tag (Cell Signaling Technology) and an anti-Actin (Sigma-Aldrich Corporation) antibody. The membranes were washed and incubated with horseradish peroxidase-conjugated secondary antibody, followed by enhanced chemiluminescence development.

Statistics

Statistical calculations were performed using Prism 4.0 (GraphPad). Differences between two variables were assessed by unpaired Student's t test. The difference was considered significant if the *P* value was less than 0.05.

Supplementary Figures

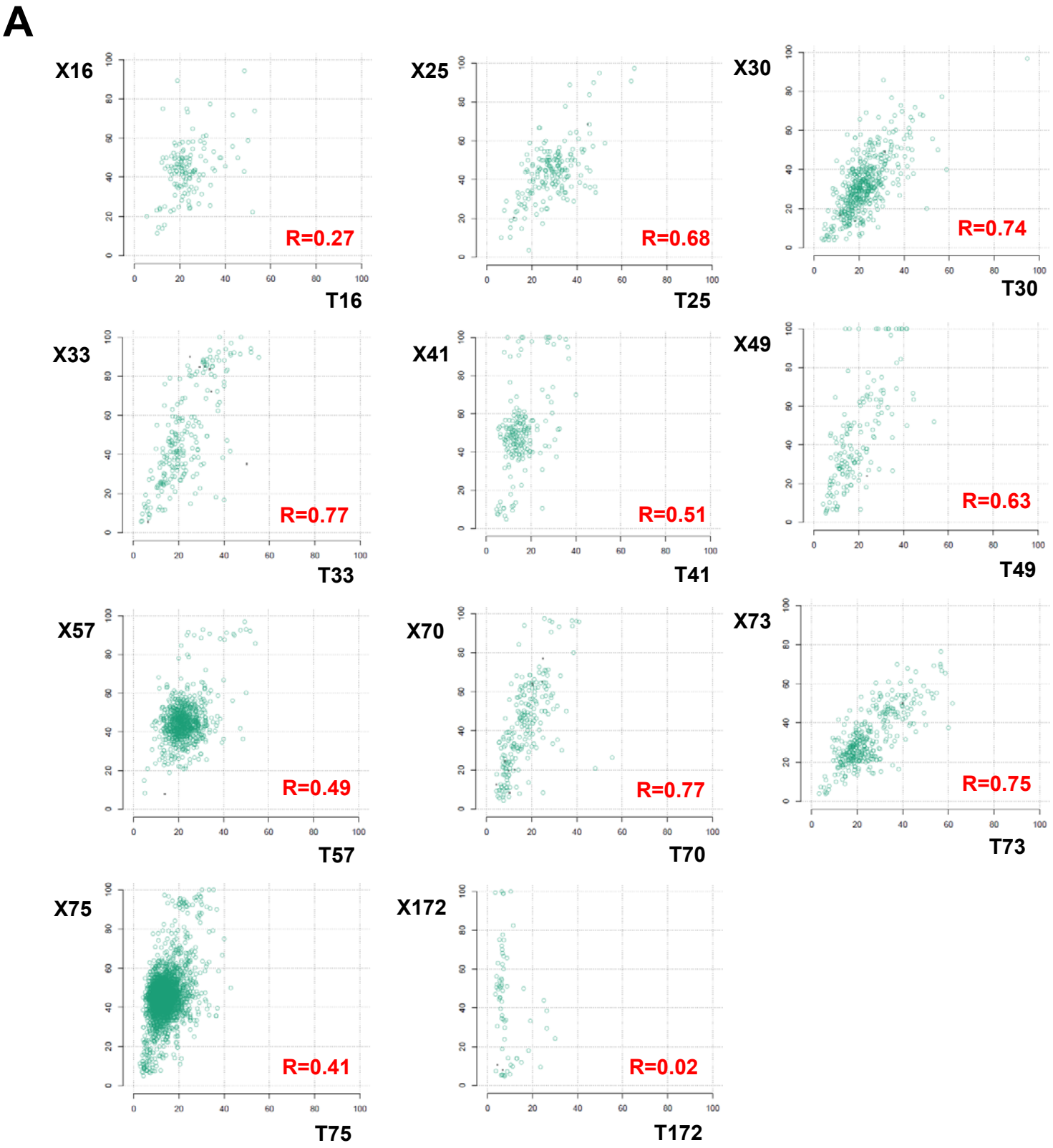

B

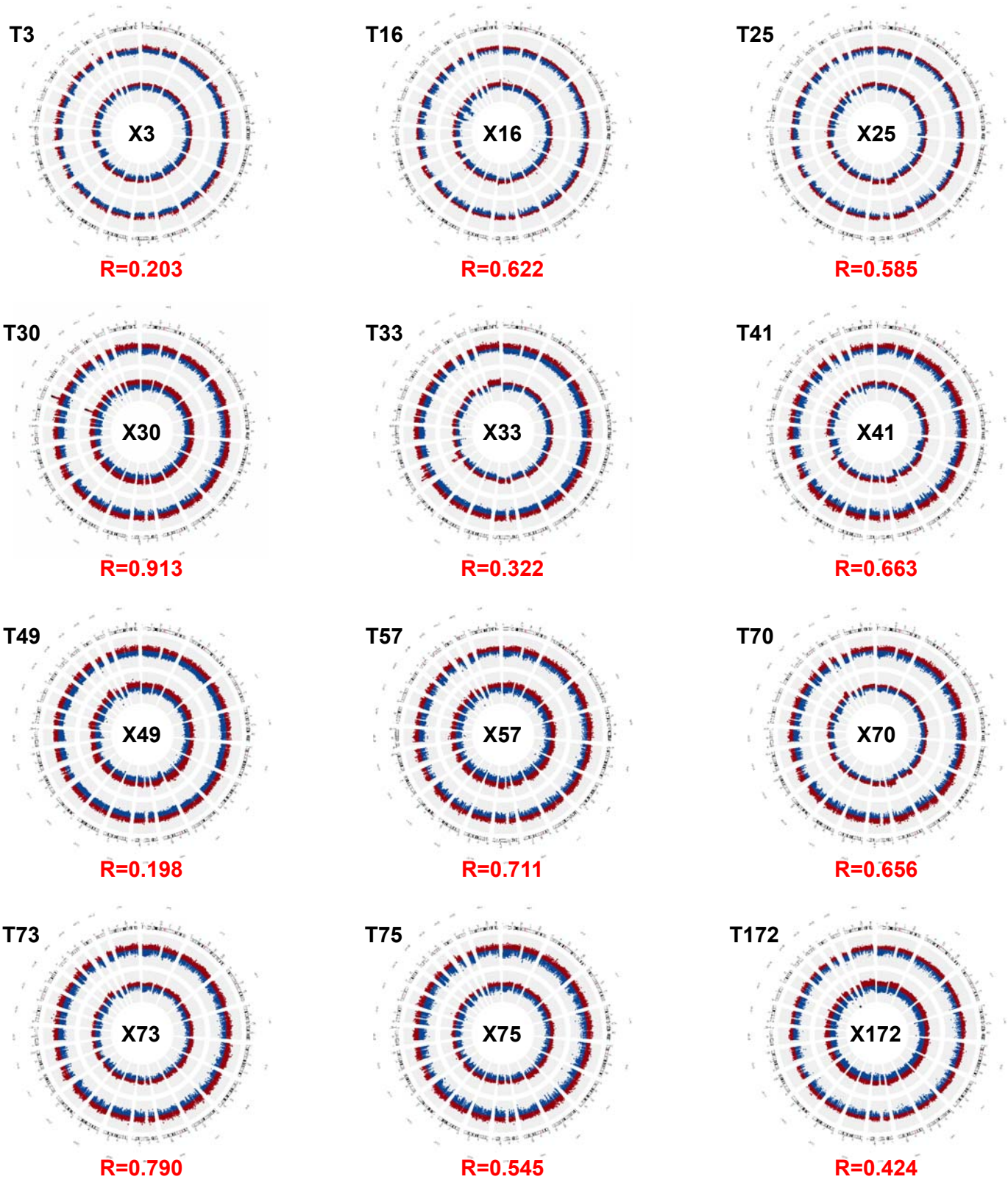
T3
X3
R=0.203
T16
X16
R=0.622
T25
X25
R=0.585
T30
X30
R=0.913
T33
X33
R=0.322
T41
X41
R=0.663
T49
X49
R=0.198
T57
X57
R=0.711
T70
X70
R=0.656
T73
X73
R=0.790
T75
X75
R=0.545
T172
X172
R=0.424

C

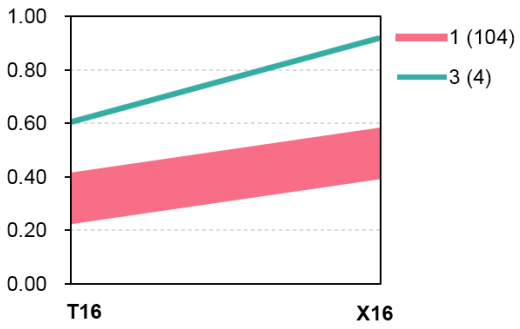
1.00
0.80
0.60
0.40
0.20
0.00
T16
X16
1 (104)
3 (4)

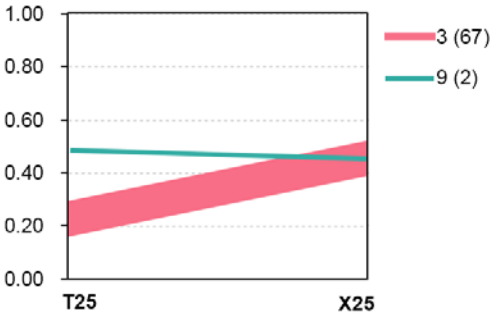
1.00
0.80
0.60
0.40
0.20
0.00
T25
X25
3 (67)
9 (2)

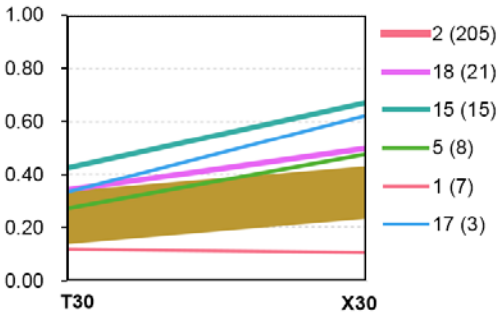
1.00
0.80
0.60
0.40
0.20
0.00
T30
X30
2 (205)
18 (21)
15 (15)
5 (8)
1 (7)
17 (3)

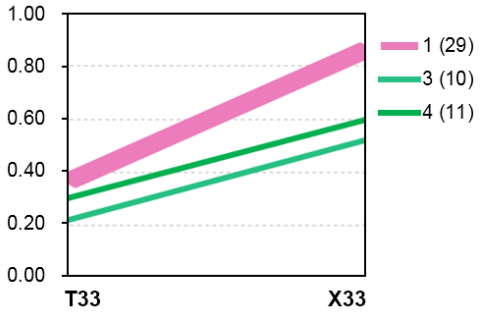
1.00
0.80
0.60
0.40
0.20
0.00
T33
X33
1 (29)
3 (10)
4 (11)

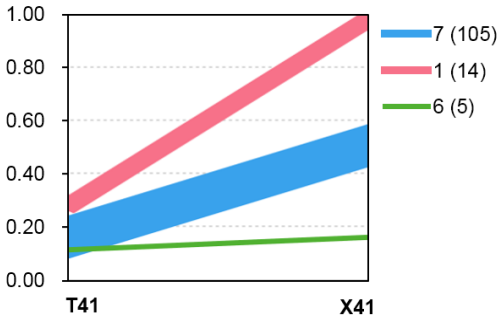
1.00
0.80
0.60
0.40
0.20
0.00
T41
X41
7 (105)
1 (14)
6 (5)

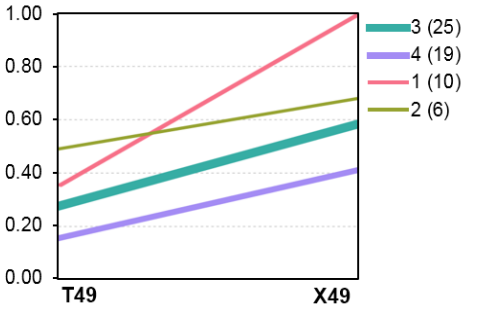
1.00
0.80
0.60
0.40
0.20
0.00
T49
X49
3 (25)
4 (19)
1 (10)
2 (6)

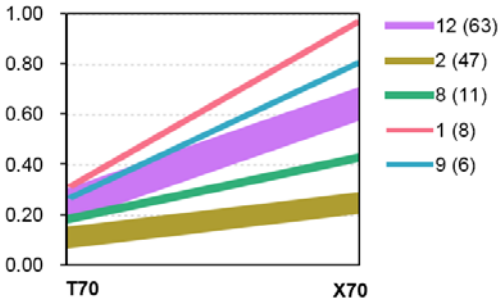
1.00
0.80
0.60
0.40
0.20
0.00
T70
X70
12 (63)
2 (47)
8 (11)
1 (8)
9 (6)

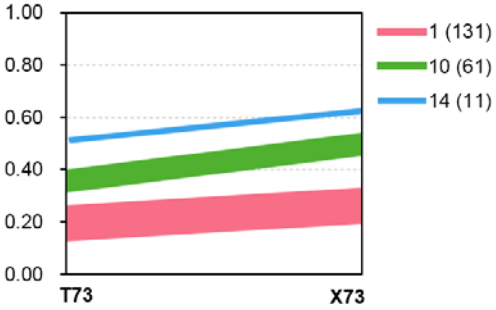
1.00
0.80
0.60
0.40
0.20
0.00
T73
X73
1 (131)
10 (61)
14 (11)

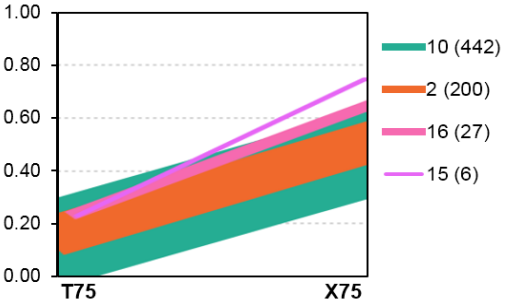
1.00
0.80
0.60
0.40
0.20
0.00
T75
X75
10 (442)
2 (200)
16 (27)
15 (6)

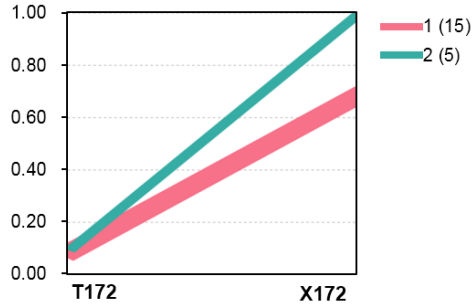
1.00
0.80
0.60
0.40
0.20
0.00
T172
X172
1 (15)
2 (5)

Supplementary Figure S1.

Genomic comparison between matched patient and PDX tumors. **A,** Comparison of somatic mutation allele frequency between matched patient and PDX tumors. The scatterplots demonstrate the distribution of somatic mutation allele frequencies of matched patient and PDX samples (T: patient tumor, X: PDX tumor). Values of Pearson correlation coefficient (R) for each pair were given in each scatterplot. **B,** Comparison of somatic copy number alterations between matched patient and PDX tumors. The plots represent genomic distribution of somatic copy number alterations in matched patient (outer circle; T) and PDX (inner circle; X) tumors. The red region indicates amplification, while the blue region indicates deletion. **C,** Comparison of clonal architecture between matched patient and PDX tumors. Plots shows tumor clonal architecture of matched patient (T) and PDX tumors (X), estimated by PyClone algorithm. Line widths indicate the number of mutations in each cluster (numbers in brackets next to each cluster).

Patient No.	Patient tissue	PDX Tissue	CEA		CK7		CK20		Ki-67		E-cadherin		Vimentin (stroma)		CD31		CD3	
			Patient	PDX	Patient	PDX	Patient	PDX	Patient	PDX	Patient	PDX	Patient	PDX	Patient	PDX	Patient	PDX
#1	T3	X3	1	2	0	0	2	3	4	4	2	3	3	0	3	0	1	1
#2	T25	X25	0	0	0	0	2	2	3	4	3	2	3	3	3	0	2	3
#5	T30	X30	2	1	0	0	2	3	4	3	2	2	3	1	3	0	3	1
#6	T58	X58	2	1	1	0	2	3	3	3	3	1	3	0	3	0	2	3
#7	T16	X16	1	1	0	0	1	2	2	3	2	3	3	2	3	0	1	3
#10	T33	X33	2	1	0	0	2	2	3	4	3	1	3	3	3	0	2	3
#13	T41	X41	1	1	0	0	1	1	3	4	2	1	3	3	3	0	2	3
#14	T49	X49	2	1	0	0	2	3	3	3	3	2	3	0	3	0	1	3
#17	T57	X57	1	1	1	1	2	1	4	4	1	1	3	3	3	0	2	3
#18	T70	X70	2	1	0	0	1	2	4	4	3	1	3	2	3	1	2	3
#19	T73	X73	1	1	0	0	2	3	3	3	3	1	3	3	3	1	3	3
#21	T75	X75	2	1	1	1	2	1	4	4	2	1	3	3	3	1	2	3
#27	T106	X106	1	2	0	1	1	2	3	3	2	2	3	1	3	0	1	3
#34	T167	X167	1	1	0	0	1	2	3	3	2	3	3	1	3	1	3	3
#35	T172	X172	2	0	0	0	1	1	2	4	3	1	3	0	3	1	1	3

Supplementary Figure S2.

Summary of the immunoreactivity scores for CEA, CK7, CK20, Ki-67, E-cadherin, stromal vimentin, CD31 and CD3 in matched patient and PDX tumors.

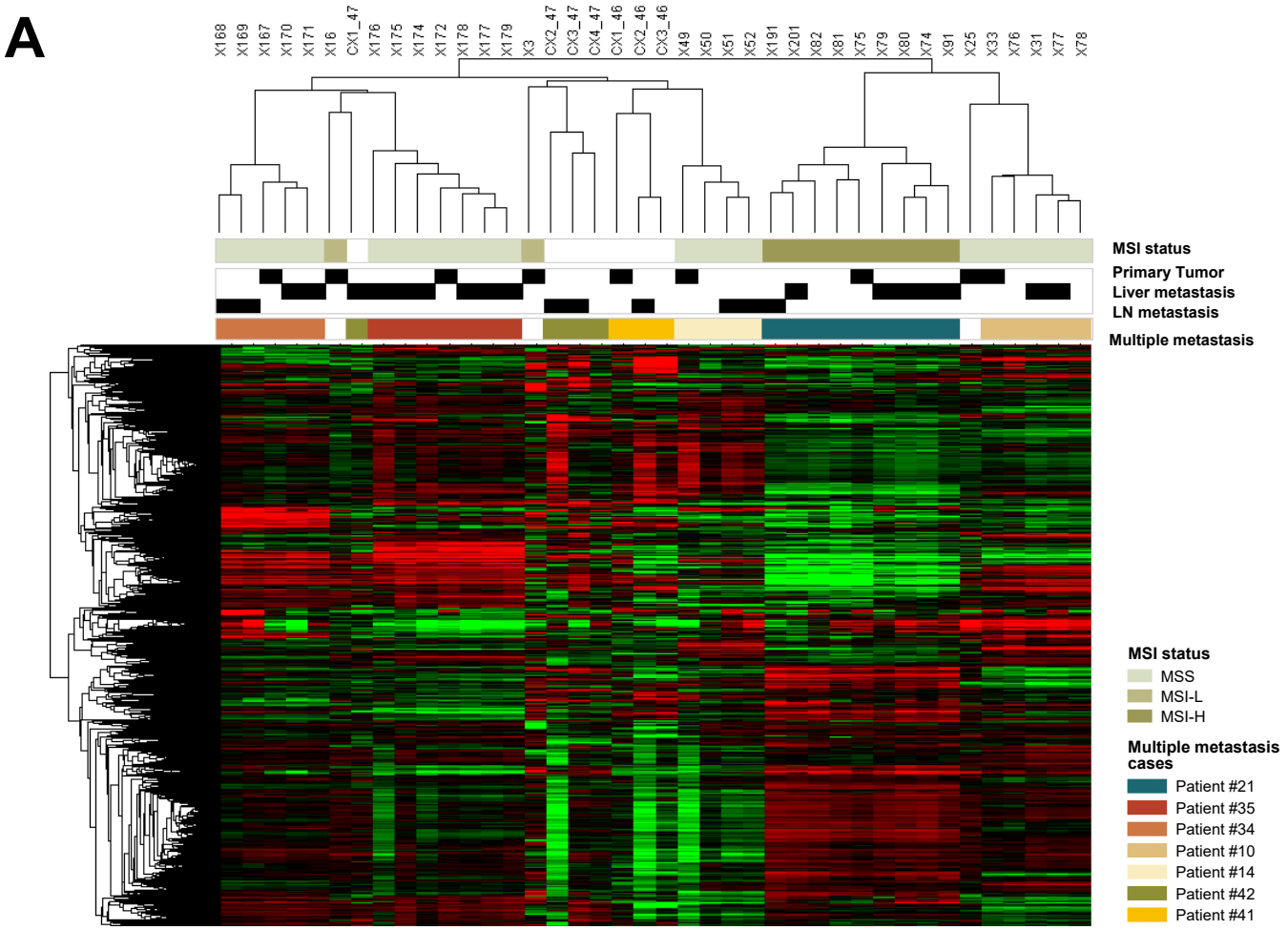
A
X168 X169 X167 X170 X171 X16 CX1_47 X176 X175 X174 X172 X178 X177 X179 X3 CX2_47 CX3_47 CX4_47 CX1_46 CX2_46 CX3_46 X49 X50 X51 X52 X191 X201 X82 X81 X75 X79 X80 X74 X91 X25 X33 X76 X31 X77 X78
MSI status
Primary Tumor
Liver metastasis
LN metastasis
Multiple metastasis
MSI status
MSS
MSI-L
MSI-H
Multiple metastasis cases
Patient #21
Patient #35
Patient #34
Patient #10
Patient #14
Patient #42
Patient #41

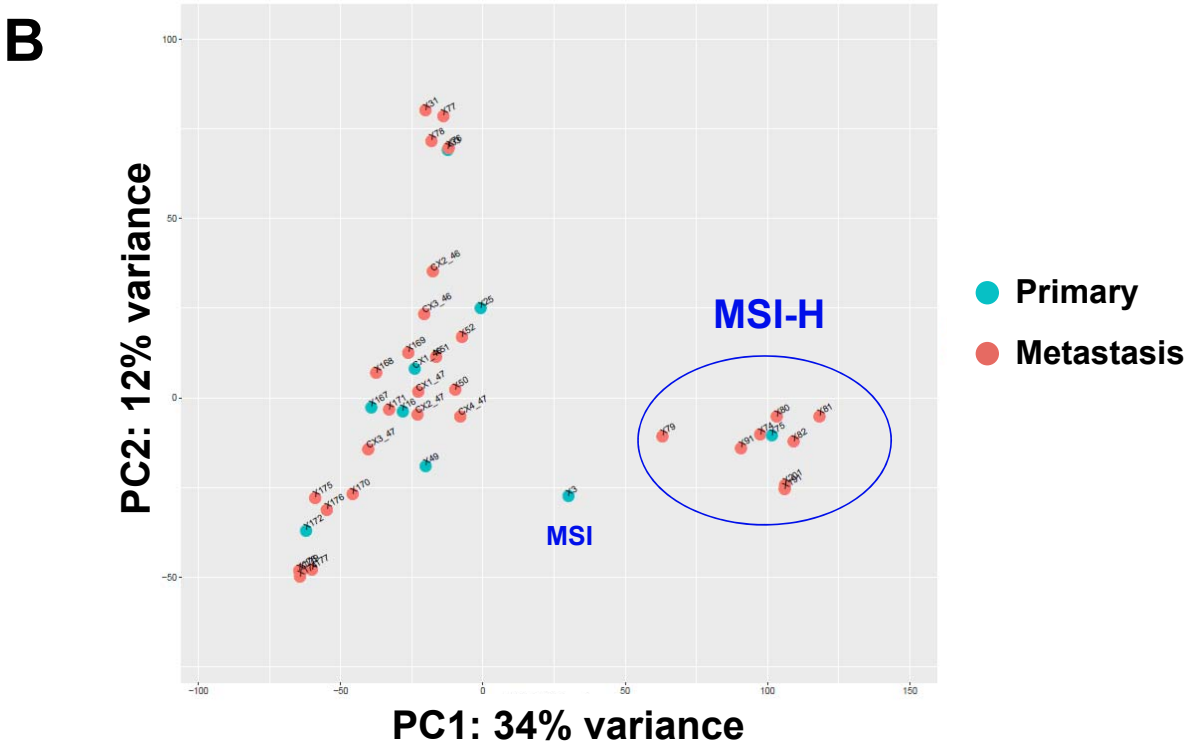
B
PC2: 12% variance
PC1: 34% variance
MSI-H
MSI
Primary
Metastasis

Supplementary Figure S3.

Transcriptomic analysis from RNA-seq data in PDX tumors of CRC patients. **A,** Hierarchical clustering of tumor samples and genes. Heatmap shows the relative expression levels of each gene (rows) in each sample (column), and rows and columns were clustered as pairwise average-linkage with Pearson distance measurement. The first five rows of heatmap designate tumor microsatellite instability (MSI) status, tumor origins (primary or metastasis) and samples from patients with multiple organ metastasis. **B,** Principal component analysis (PCA) from RNA-seq data for PDX tumors of CRC patients. PCA classified samples into two clusters of MSS and MSI-H tumors. Blue dots denote primary tumors and red dots denote metastasis tumors. MSI: microsatellite instable, MSI-H: microsatellite instable-high.

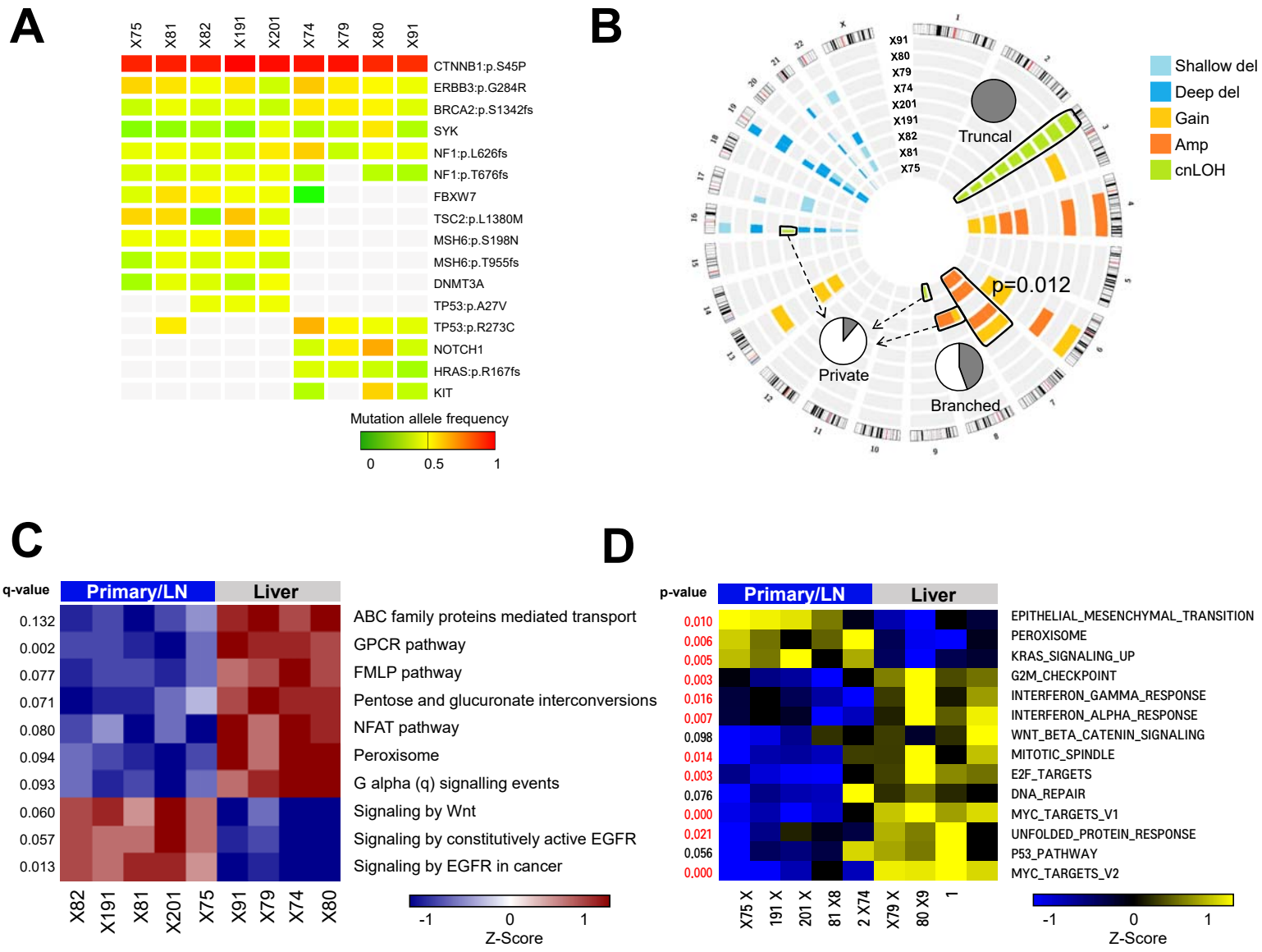

Supplementary Figure S4.

Genomic and transcriptomic heterogeneity of primary and metastasized tumors from a CRC patient with microsatellite instability-high status. **A,** Regional distribution of somatic mutations on cancer-related genes. Heatmap shows the regional distribution of mutations on cancer-related genes and mutant-allele frequencies. The selection criteria of cancer-related genes are described in Methods. The somatic variants are shown as rows on the heatmap, and the mutant allele frequency of each variant was expressed in color gradient. **B,** Schematic representation of copy number alterations (CNAs). Each color represent each type of CNAs described in legend, and representative examples of truncal, branched and private alterations were depicted in the figure. **C,** Pathway analysis for differentially expressed genes between primary/LN group and liver-metastasized groups. Heatmap shows the relative values of each pathway gene signature (rows) in each sample (column). **D,** Pathway analysis for differentially promoter-methylated genes between primary/LN group and liver-metastasized groups. Heatmap shows the relative values of each pathway gene signature (rows) in each sample (column).

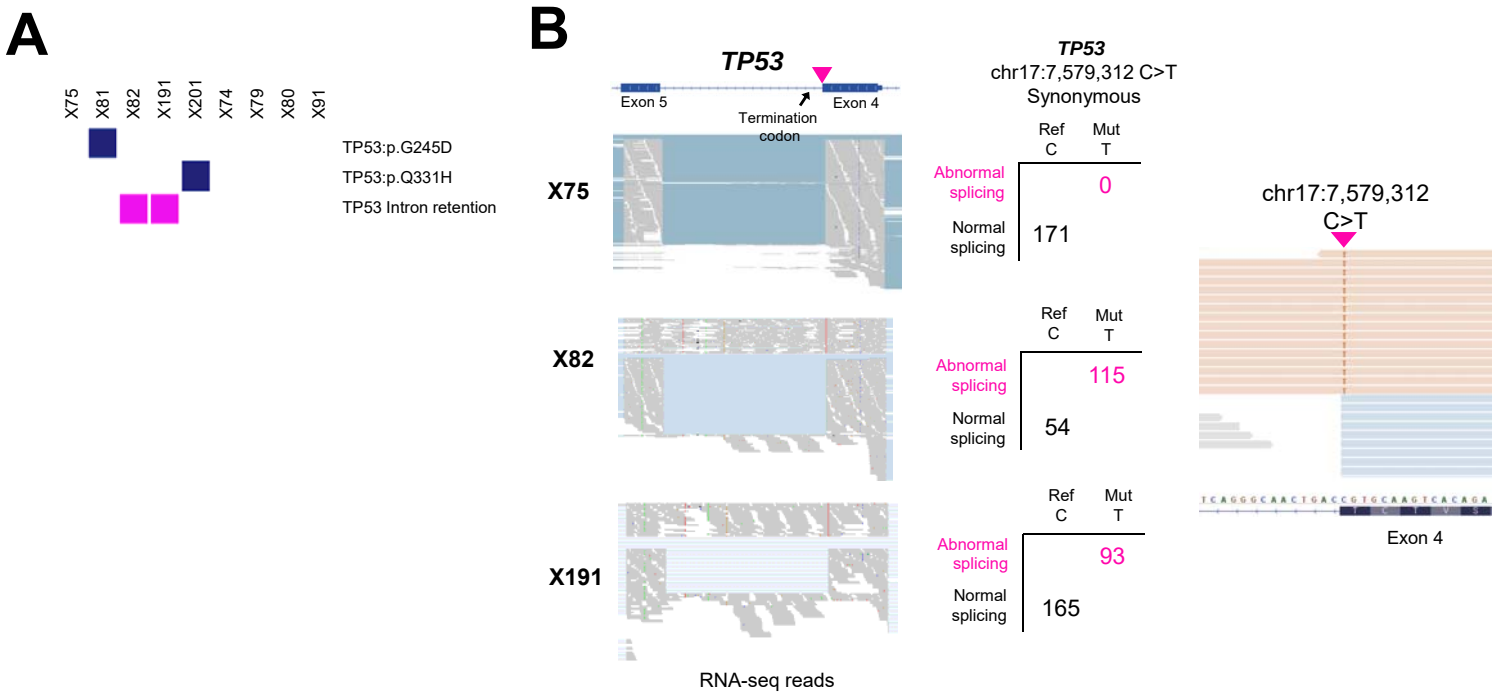

Supplementary Figure S5.

Convergent bi-allelic inactivation of *TP53* gene in metastatic tumors in lymph node-metastasis group. **A,** Second-hit for bi-allelic *TP53* inactivation in LN tumor group of patient #21. **B,** Synonymous mutation on intron-exon boundary and intron retention of *TP53* in X82 and X191.

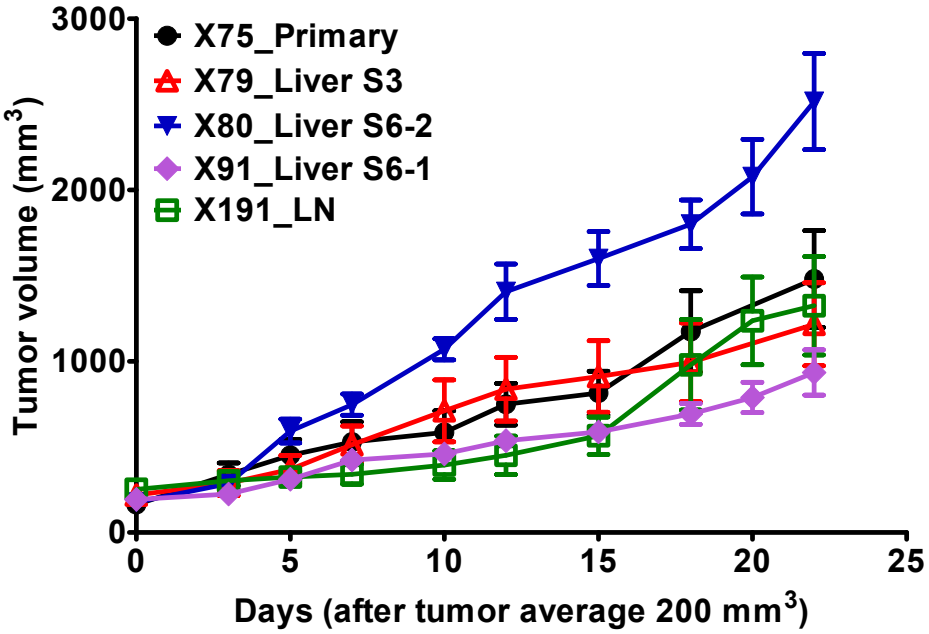

Supplementary Figure S6.

Tumor growth curve of PDXs from multiple organ metastasis in patient #21. The graph shows the average tumor size for vehicle-treated mice of each group (n = 5) after the average size of tumors reached 200 mm^3.

A

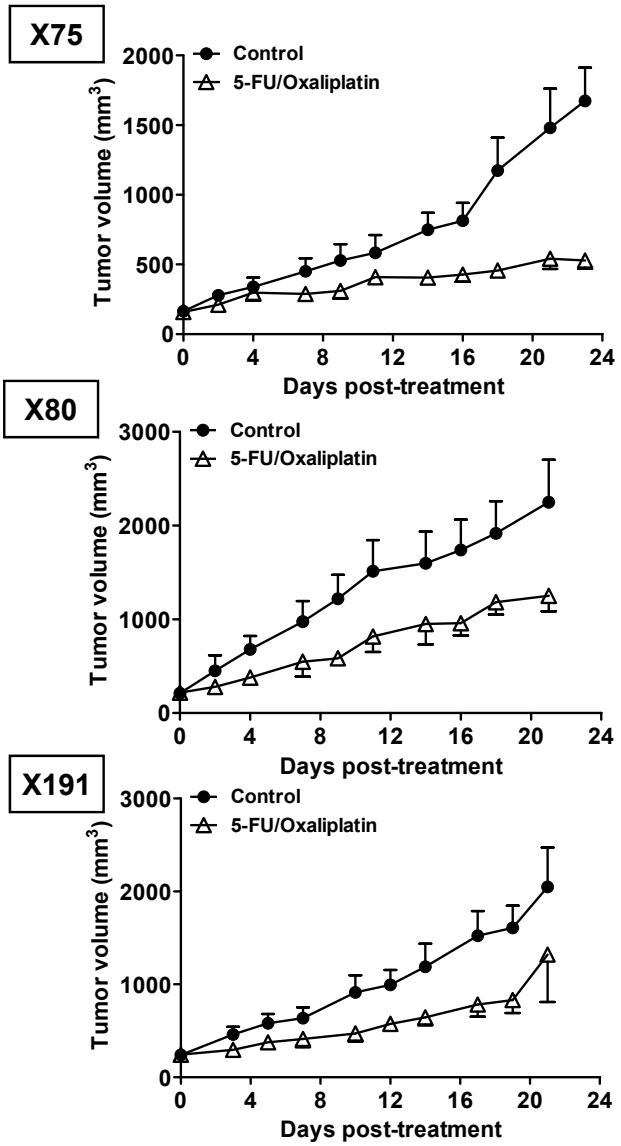
X75
Control
5-FU/Oxaliplatin
Tumor volume (mm3)
Days post-treatment
X80
Control
5-FU/Oxaliplatin
Tumor volume (mm3)
Days post-treatment
X191
Control
5-FU/Oxaliplatin
Tumor volume (mm3)
Days post-treatment

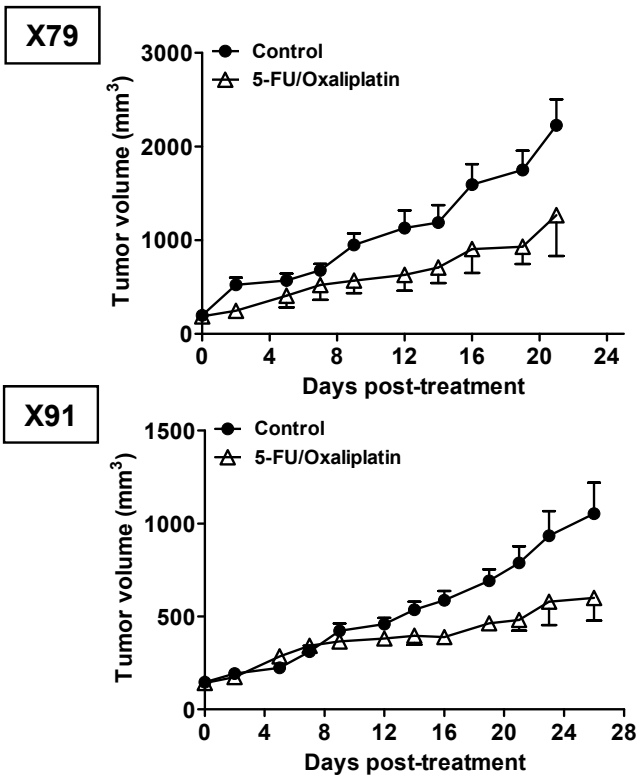
X79
Control
5-FU/Oxaliplatin
Tumor volume (mm3)
Days post-treatment
X91
Control
5-FU/Oxaliplatin
Tumor volume (mm3)
Days post-treatment

B

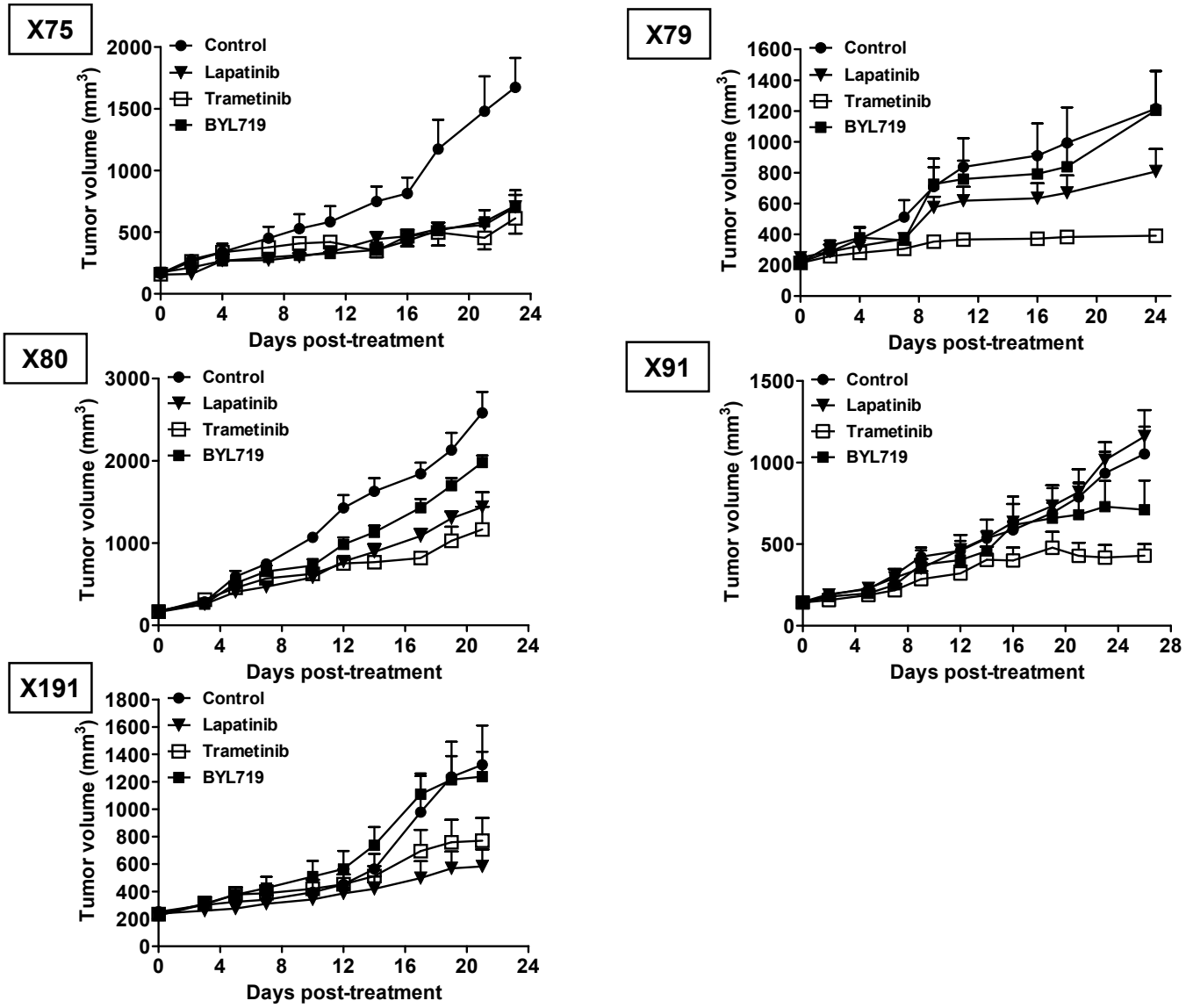

Supplementary Figure S7.

In vivo treatment efficacy in PDX models from multiple organ metastasis of patient #21. **A,** *In vivo* efficacy of 5-FU + oxaliplatin in PDX models from patient #21. Mice with PDXs were treated with vehicle or 5-FU (50 mg/kg/week) + oxaliplatin (5 mg/kg/week) (5-FU/Oxaliplatin) for 21 -26 days depending on sample conditions. Average tumor sizes for each group are plotted. **B,** *In vivo* efficacy of lapatinib, trametinib and BYL719 in PDX models from patient #21. Mice with PDXs were treated with lapatinib (30 mg/kg, twice a day), trametinib (2 mg/kg/day), and BYL719 (25 mg/kg/day) for 21 -26 days depending on sample conditions. Average tumor sizes for each group are plotted.

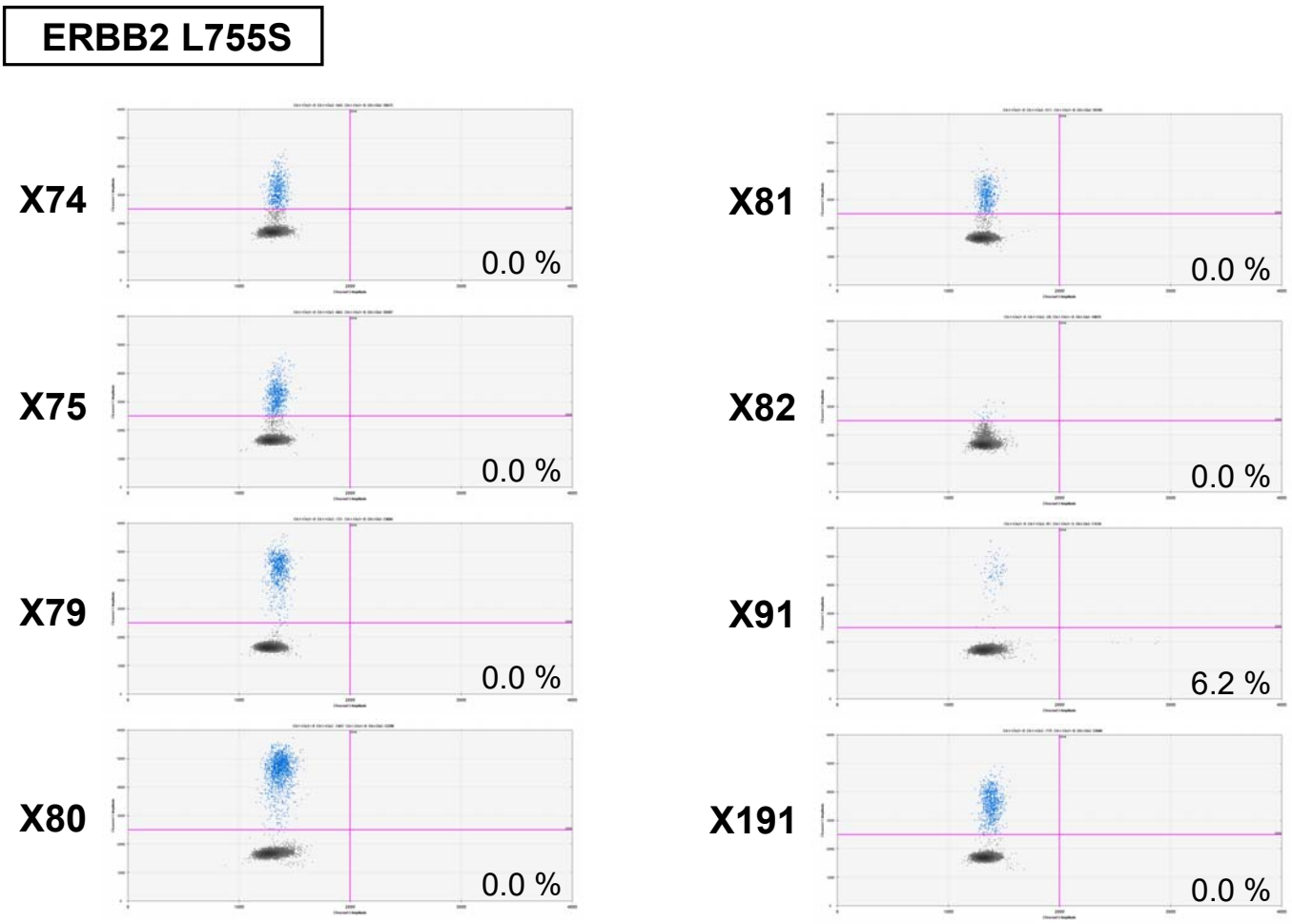

Supplementary Figure S8.

Detection of ERBB2 L755S mutations using droplet digital PCR (ddPCR). Multiplex ddPCR was performed for wild-type ERBB2 (blue dots) and mutant ERBB2 (L755S; green dots) using tumor DNA from primary and metastasis tumors. The numbers besides the graphs indicate the allele frequency of mutant ERBB2.

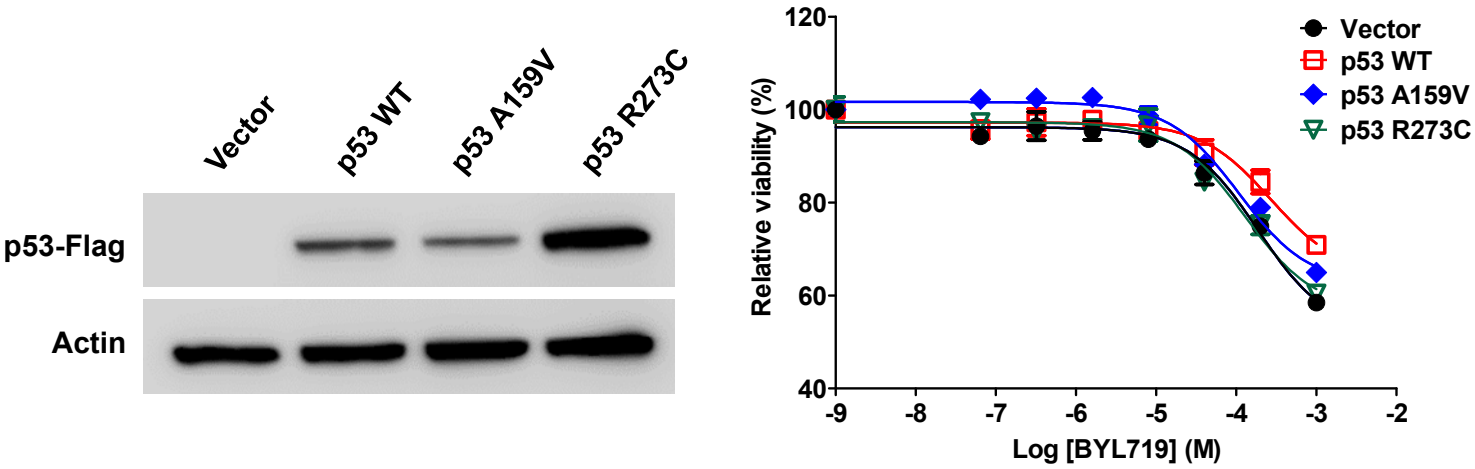

Supplementary Figure S9.

The effect of *TP53* mutations on sensitivity to a PI3K inhibitor, BYL719, in HEK293 cells. Wild-type (WT) and mutant (A159V, R273C) of *TP53* was over-expressed in HEK293 cells (right panel), and WST assays were used to examine the cytotoxic effect after 72 h treatment of BYL719 in each concentration (left panel).

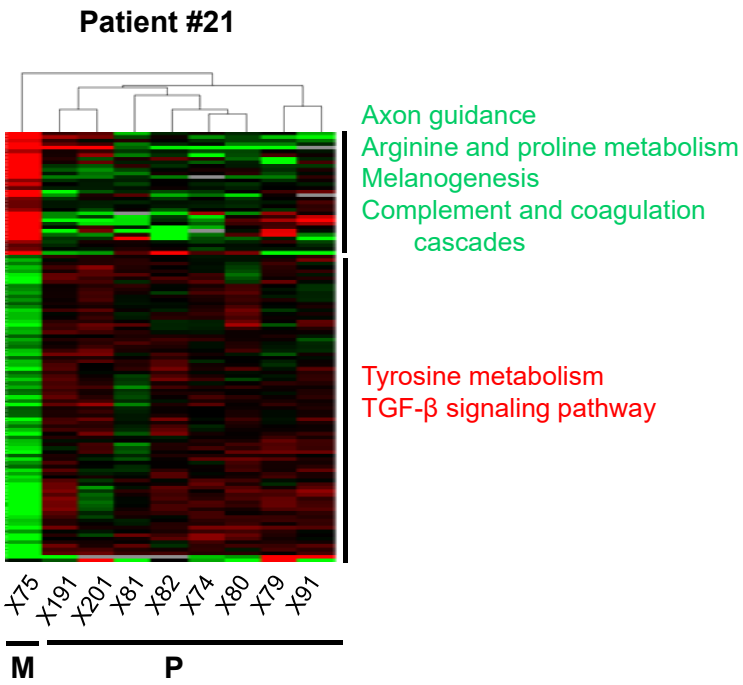

Supplementary Figure S10.

Metastasis-specific altered pathways from transcriptomic analysis in PDX tumors of patient #21. Differentially expressed genes (DEGs) between primary and metastasis PDX tumors were hierarchically clustered and illustrated in a heat map (P, primary; M, metastasis). The enriched pathways in DEGs were depicted adjacent to heat map in green letters for primary tumors and red letters for metastasis tumors. Genes with adjusted *P*-value < 0.05 were used for pathway analysis.

Supplementary Table S1. Clinical information for CRC patients.

Patient ID	Sex	Age	T stage	N stage	M stage	Stage	MSI status	KRAS 12	KRAS 13	Chemotherapy	Chemosensitivity	Recurrence sites
#1	M	47	4	2	1	IV	MSI-L	Wild	p.G13V (c.38_39GC>TT)	FOLFOX	PD	Peritoneal seeding
#2	F	69	3	1	0	III	MSS	Wild	Wild	CCRT (LF)	SD	
#3	F	79	3	1	0	III	MSS	Wild	Wild	XELODA	SD	
#4	M	74	2	2	0	III	MSS	Wild	Wild	XELODA	SD	
#5	F	42	2	0	0	I	MSS	Wild	Wild	No chemo	—	
#6	M	66	3	0	0	II	MSS	Wild	p.G13D (c.38 G>A)	XELODA	SD	
#7	F	87	3	2	0	III	MSI-L	N/A	Wild	No chemo	—	
#8	F	85	4	0	0	II	MSS	Wild	p.G13D (c.38 G>A)	No chemo	—	
#9	M	66	3	0	0	II	MSI-L	Wild	Wild	No chemo	—	
#10	M	74	4	1	1	IV	MSS	Wild	Mutant	No chemo	—	
#11	F	73	3	0	0	II	MSS	Wild	p.G13D (c.38 G>A)	No chemo	—	
#12	M	58	3	0	1	IV	MSS	Wild	Wild	FOLFIRI, cetuximab	SD	
#13	M	78	3	1	1	IV	MSS	Wild	Wild	No chemo	—	Liver
#14	F	54	4	2	1	IV	MSS	Wild	Wild	FOLFIRI, cetuximab → FOLFOX6	PR → PD	Liver → LN, ovary, liver
#15	F	81	4	2	1	IV	MSS	p.G12S (c.34G>A)	Wild	No chemo	PD	Liver, peritoneal seeding
#16	F	55	3	1	1	IV	MSS	Wild	Wild	CCRT (LF) → FOLFOX	PD → SD	Liver
#17	M	40	3	0	0	II	MSS	Wild	Wild	No chemo	—	
#18	M	50	4	2	0	III	MSS	Wild	Wild	FOLFOX	SD	
#19	M	69	2	0	0	I	MSS	Wild	Wild	No chemo	—	
#20	M	58	4	1	1	IV	MSS	Wild	Wild	N/A	—	
#21	M	48	4	2	1	IV	MSI-H	Wild	Wild	FOLFIRI, cetuximab	PD	Liver, adrenal, LN
#22	M	66	3	0	1	IV	MSS	Wild	Wild	FOLFIRI, cetuximab	SD	
#23	M	52	4	0	0	II	MSS	Wild	Wild	CCRT (LF)	SD	

#24	F	88	3	2	1	IV	N/A	N/A	N/A	No chemo	—	
#25	M	55	4	1	1	IV	MSS	Wild	Wild	FOLFIRI, cetuximab	CR	
#26	F	65	—	—	1	IV	MSS	Wild	Wild	FOLFIRI, cetuximab	PR → PD	Liver
#27	M	69	3	1	0	III	MSS	Wild	Wild	XELOX	SD	
#28	M	58	3	1	1	IV	MSS	p.G12V (c.35G>T)	Wild	Avastine, FOLFIRI	SD	
#29	M	48	3	1	0	III	MSS	Wild	Wild	XELOX	SD	
#30	M	78	4	1	0	III	MSS	Wild	Wild	Capecitabine	SD	
#31	M	79	3	1	0	III	MSS	Mutant	Wild	No chemo	—	
#32	F	83	3	1	1	IV	MSS	Mutant	Wild	No chemo	—	
#33	M	55	3	1	1	IV	MSS	Wild	Wild	FOLFIRI, cetuximab	SD	
#34	M	60	3	1	1	IV	MSS	Mutant	Wild	No chemo	PD	
#35	F	51	3	1	1	IV	MSS	Mutant	Wild	Avastine, FOLFIRI	PR	
#36	F	42	3	0	0	II	MSS	Mutant	Wild	LF	SD	
#37	M	56	4	1	1	IV	MSS	Wild	Wild	FOLFIRI, cetuximab	SD	
#38	M	55	3	0	1	IV	MSS	Mutant	Wild	Cetuximab → XRT with LF	—	
#39	M	33	—	—	—	—	N/A	N/A	N/A	N/A	—	
#40	M	78	3	1	1	IV	MSS	Wild	Wild	CCRT (Xeloda)	—	Liver
#41	M	67	—	—	—	—	MSS	N/A	N/A	N/A	—	
#42	M	55	—	—	—	—	MSS	Wild	Wild	N/A	—	
#43	F	53	4	2	1	IV	MSS	Wild	Wild	FOLFIRI	PD	ovary, para-aortic
#44	F	51	4	2	1	IV	MSS	Wild	Wild	Cetuximab + FOLFOX	CR → PD	Liver, ovary, peritoneum
#45	F	59	3	2	1	IV	MSS	Gly12 Val (c.35G>T)	Wild	Avastine + FOLFOX	SD → PD	liver
#46	M	73	3	—	—	—	N/A	—	—	—	—	
#47	F	48	3	2	1	IV	MSS	Wild	Wild	FOLFOX	CR	ovary

Supplementary Table S2. Sample lists for PDX generation and genomic analysis.

Patient ID	Tumor type	Tumor site	PDX trial	PDX generation	Patient tumor WES	Patient tumor WES ID	PDX tumor WES	PDX tumor WES ID	PDX tumor RNA-seq	PDX tumor RNA-seq ID	PDX tumor methyl-seq	PDX tumor methyl-seq ID
#1	Primary	A colon	V	V	V	T3	V	X3	V	X3		
#2	Primary	Rectum	V	V	V	T25	V	X25	V	X25		
#3	Primary	S colon	V									
#4	Primary	RS colon	V									
#5	Primary	A colon	V	V	V	T30	V	X30				
#6	Primary	S colon	V	V	V	T58	V	X58				
#7	Primary	S colon	V	V	V	T16	V	X16	V	X16		
#8	Primary	S colon	V	V			V	X137				
#9	Primary	RS colon	V									
#10	Primary	RS colon	V	V	V	T33	V	X33	V	X33	V	X33
	Metastatic	Liver S2	V	V	V	T31	V	X31	V	X31	V	X31
	Metastatic	Mesenteric	V	V	V	T76	V	X76	V	X76	V	X76
	Metastatic	Liver S8	V	V	V	T77	V	X77	V	X77	V	X77
	Metastatic	Peritoneum	V	V	V	T78	V	X78	V	X78	V	X78
#11	Primary	A colon	V	V			V	X83				
#12	Primary	S colon	V		V	T159						
	Metastatic	Liver	V									
#13	Primary	Rectum	V	V	V	T41	V	X41				
#14	Primary	Rectum	V	V	V	T49	V	X49	V	X49	V	X49
	Metastatic	Ovary	V	V	V	T50	V	X50	V	X50	V	X50
	Metastatic	LN (perocolic)	V	V	V	T51	V	X51	V	X51	V	X51
	Metastatic	LN (paraaortic)	V	V	V	T52	V	X52	V	X52	V	X52
#15	Metastatic	Omentum	V	V	V	T42	V	X42				
	Metastatic	Peritoneum	V	V	V	T56	V	X56				
#16	Metastatic	Liver	V	V	V	T43	V	X43				
#17	Primary	HF colon	V	V	V	T57	V	X57				
#18	Primary	D colon	V	V	V	T70	V	X70				
	Metastatic	LN	V		V	T190						
#19	Primary	HF colon	V	V	V	T73	V	X73				
	Metastatic	Stomach	V		V	T189						
#20	Primary	S colon	V									
	Metastatic	Liver	V	V	V	T146						
#21	Primary	A colon	V	V	V	T75	V	X75	V	X75	V	X75
	Metastatic	LN	V	V	V	T191	V	X191	V	X191	V	X191
	Metastatic	Liver S3	V	V	V	T79	V	X79	V	X79	V	X79
	Metastatic	Liver S6-1	V	V	V	T91	V	X91	V	X91	V	X91
	Metastatic	Liver S6-2	V	V	V	T80	V	X80	V	X80	V	X80
	Metastatic	Liver S8	V	V	V	T74	V	X74	V	X74	V	X74
	Metastatic	Omentum	V	V	V	T81	V	X81	V	X81	V	X81

	Metastatic	Mesenteric	V	V	V	T82	V	X82	V	X82	V	X82
	Metastatic	Liver	V	V			V	X201	V	X201	V	X201
#22	Primary	D colon	V	V			V	X147				
#23	Primary	Rectum	V	V			V	X109				
#24	Primary	Rectum	V									
	Metastatic	LN	V		V	T188						
#25	Primary	RS colon	V		V	T161						
	Metastatic	LN	V		V	T162						
#26	Primary	A colon	V	V	V	T149						
	Metastatic	LN	V									
	Metastatic	Mesenteric	V		V	T187						
	Metastatic	Omentum	V	V	V	T143						
#27	Primary	S colon	V	V	V	T106	V	X106				
	Metastatic	Stomach	V	V	V	T186						
#28	Primary	S colon	V	V	V	T185						
	Metastatic	Liver	V	V	V	T140						
#29	Primary	RS colon	V	V	V	T155						
	Metastatic	LN	V		V	T184						
#30	Primary	HF colon	V		V	T163						
	Metastatic	LN	V		V	T164						
#31	Primary	RS colon	V	V	V	T165						
	Metastatic	LN	V	V	V	T166						
#32	Primary	S colon	V	V	V	T153						
	Metastatic	Liver	V		V	T181						
	Metastatic	LN	V	V	V	T182						
#33	Primary	S colon	V	V	V	T154						
	Metastatic	Liver	V	V	V	T180						
#34	Primary	A colon	V	V	V	T167	V	X167	V	X167		
	Metastatic	LN (SMV)	V	V	V	T168	V	X168	V	X168		
	Metastatic	LN (pericolic)	V	V	V	T169	V	X169	V	X169		
	Metastatic	Liver S2	V	V	V	T170	V	X170	V	X170		
	Metastatic	Liver S4	V	V	V	T171	V	X171	V	X171		
#35	Primary	Rectum	V	V	V	T172	V	X172	V	X172		
	Metastatic	Liver S2	V		V	T173						
	Metastatic	Liver S2-2	V	V			V	X174	V	X174		
	Metastatic	Liver S6	V	V	V	T175	V	X175	V	X175		
	Metastatic	Liver S7	V	V	V	T176	V	X176	V	X176		
	Metastatic	Liver S8	V	V	V	T177	V	X177	V	X177		
	Metastatic	Liver S5/6	V	V	V	T178	V	X178	V	X178		
	Metastatic	Liver S6-3	V	V	V	T179	V	X179	V	X179		
#36	Primary	RS colon	V	V								
#37	Primary	RS colon	V	V								
	Metastatic	LN	V									
#38	Metastatic	Liver	V	V								
#39	Primary	Colon (FAP)	V	V			V	CX_43				

#40	Primary	Rectum	V							
	Metastatic	Liver	V	V						
#41	Primary	Rectum	V	V			V	CX1_46	V	CX1_46
	Metastatic	LN	V	V			V	CX2_46	V	CX2_46
	Metastatic	Peritoneum	V	V			V	CX3_46	V	CX3_46
	Metastatic	Lung	V							
#42	Metastatic	Liver	V	V			V	CX1_47	V	CX1_47
	Metastatic	N (peripancreati	V	V			V	CX2_47	V	CX2_47
	Metastatic	LN (pericolic)	V	V			V	CX3_47	V	CX3_47
	Metastatic	LN (paraaortic)	V							
	Metastatic	Omentum	V	V			V	CX4_47	V	CX4_47
#43	Primary	S colon			V	CT_101				
	Metastatic	Ovary			V	COv_101				
#44	Primary	S colon			V	CT_102				
	Metastatic	Ovary			V	COv_102				
#45	Primary	A colon			V	CT_103				
	Metastatic	Ovary			V	COv_103				
#46	Primary	Colon			V	CT_104				
	Metastatic	Ovary			V	COv_104				
#47	Primary	S colon			V	CT_105				
	Metastatic	Ovary			V	COv_105				

* A colon - ascending colon, HF colon - hepatic flexure colon, T colon -transverse colon, D colon - descending colon, S colon - sigmoid colon, RS colon - rectosigmoid colon

Supplementary Table S3. Summary of PDX engraftment rates.

	PDX trial	PDX generation	PDX engraftment rate (%)	*P* -value
Primary	**38**	**29**	**76.3**	
(1) Primary tumor site				
A colon	6	6	100.0	0.5362
D colon	2	2	100.0	
HF colon	3	2	66.7	
Rectum	8	6	75.0	
RS colon	8	5	62.5	
S colon	10	7	70.0	
Colon (total)	1	1	100.0	
(2) Tumor stage				
I	2	2	100.0	0.8815
II	7	6	85.7	
III	9	6	66.7	
IV	18	13	72.2	
N/A	2	2	100.0	
(3) MSI status				
MSS	32	25	78.1	1
MSI	4	3	75.0	
N/A	2	1	50.0	
Metastasis	**57**	**43**	**75.4**	
(1) Metastasis sites				
Liver	25	22	88.0	0.5954
LN	18	10	55.6	
Ometum/peritoneum/ Mesentery	10	9	90.0	
Ovary	1	1	100.0	
Lung	1	0	0.0	
Stomach	2	1	50.0	

Supplementary Table S4. Summary of clonal evolution anlaysis using PyClone.

	cluster_id (size)	Average changes upon metastasis in pt	Average changes upon metastasis in pdx	Average changes upon engraftment	T33	T31	T76	T77	T78	X33	X31	X76	X77	X78
Patient #10	1 (29)	-0.174	0.031	0.672	0.36	0.21	0.20	0.11	0.23	0.87	0.96	0.88	0.85	0.91
	3 (10)	-0.074	0.052	0.409	0.22	0.18	0.11	0.10	0.17	0.52	0.68	0.50	0.56	0.56
	4 (11)	-0.119	0.114	0.490	0.30	0.17	0.23	0.10	0.21	0.60	0.71	0.73	0.69	0.73
		-0.122	**0.066**	**0.523**										

	cluster_id (size)	Average changes upon metastasis in pt	Average changes upon metastasis in pdx	Average changes upon engraftment	T49	T50	T51	T52	X49	X50	X51	X52
Patient #14	3 (25)	0.063	0.021	0.274	0.28	0.56	0.19	0.28	0.58	0.67	0.57	0.57
	4 (19)	0.062	-0.066	0.160	0.16	0.37	0.13	0.17	0.41	0.42	0.33	0.30
	1 (10)	0.164	-0.045	0.485	0.36	0.87	0.28	0.41	1.00	0.99	0.95	0.91
	2 (6)	0.103	-0.034	0.086	0.49	0.66	0.34	0.79	0.68	0.69	0.60	0.66
		0.098	**-0.031**	**0.251**								

	cluster_id (size)	Average changes upon metastasis in pt	Average changes upon metastasis in pdx	Average changes upon engraftment	T75	T81	T82	T191	T79	T74	T80	T91	X75	X81	X82	X191	X201	X79	X74	X80	X91
Patient #21	10 (442)	0.109	0.015	0.204	0.15	0.13	0.34	0.21	0.16	0.31	0.24	0.42	0.46	0.48	0.47	0.48	0.48	0.49	0.47	0.47	0.46
	2 (200)	0.128	0.019	0.201	0.18	0.18	0.39	0.28	0.21	0.36	0.28	0.46	0.50	0.51	0.54	0.53	0.53	0.53	0.51	0.51	0.51
	16 (27)	0.091	-0.095	0.203	0.24	0.23	0.50	0.37	0.18	0.34	0.27	0.43	0.64	0.65	0.51	0.68	0.57	0.50	0.48	0.49	0.49
	15 (6)	0.159	-0.057	0.283	0.23	0.18	0.56	0.32	0.21	0.48	0.43	0.56	0.75	0.93	0.61	0.93	0.70	0.61	0.62	0.52	0.61
		0.122	**-0.030**	**0.223**																	

	cluster_id (size)	Average changes upon metastasis in pt	Average changes upon metastasis in pdx	Average changes upon engraftment	T167	T168	T169	T170	T171	X167	X168	X169	X170	X171
Patient #34	2 (24)	-0.228	-0.003	0.248	0.46	0.13	0.32	0.32	0.15	0.53	0.52	0.52	0.58	0.47
	1 (23)	-0.135	-0.014	0.161	0.28	0.08	0.18	0.20	0.11	0.34	0.32	0.32	0.36	0.31
	3 (16)	-0.262	-0.029	0.334	0.54	0.13	0.35	0.42	0.19	0.68	0.67	0.65	0.70	0.61
		-0.208	**-0.016**	**0.248**										

	cluster_id (size)	Average changes upon metastasis in pt	Average changes upon metastasis in pdx	Average changes upon engraftment	T172	T173	T175	T176	T177	T178	T179	X172	X174	X175	X176	X177	X178	X179
Patient #35	1 (15)	0.064	0.004	0.537	0.09	0.10	0.11	0.19	0.26	0.15	0.13	0.68	0.62	0.63	0.65	0.52	0.69	0.99
	2 (5)	0.149	0.007	0.764	0.10	0.11	0.14	0.38	0.44	0.22	0.22	0.99	1.00	0.98	0.99	1.00	1.00	1.00
		0.107	**0.006**	**0.650**														

	cluster_id (size)	Average changes upon metastasis in pt	T153	T181	T182
Patient #26	10 (99)	-0.032	0.40	0.37	0.36
	4 (12)	-0.112	0.69	0.59	0.58
	1 (7)	-0.097	0.86	0.78	0.75
		-0.080			

	cluster_id (size)	Average changes upon metastasis in pt	T149	T143	T187
Patient #32	1 (70)	0.008	0.23	0.22	0.26
	6 (55)	0.025	0.40	0.39	0.45
	5 (9)	0.008	0.55	0.56	0.56
		0.014			

	cluster_id (size)	Average changes upon metastasis in pdx	CX1_46	CX2_46	CX3_46
Patient #41	5 (44)	0.156	0.49	0.66	0.64
	9 (26)	-0.071	0.53	0.45	0.47
	2 (21)	0.017	0.98	0.99	1.00
	7 (12)	-0.080	0.40	0.27	0.37
		0.005			

	cluster_id (size)	Average changes in pdx	CX1_47	CX2_47	CX3_47	CX4_47
Patient #42	13 (54)	-0.019	0.63	0.61	0.62	0.58
	3 (42)	0.056	0.40	0.43	0.49	0.45
	17 (32)	-0.361	0.97	0.64	0.59	0.59
	9 (19)	-0.277	0.66	0.42	0.38	0.36
	2 (9)	0.010	0.93	0.97	1.00	0.85
		-0.118				

	cluster_id (size)	Average changes in pdx	T16	X16
Patient #7	1 (104)	0.166	0.32	0.49

	cluster_id (size)	Average changes in pdx	T25	X25
Patient #2	3 (67)	0.218	0.24	0.45

	cluster_id (size)	Average changes in pdx	T30	X30
Patient #5	2 (205)	0.094	0.24	0.33
	18 (21)	0.154	0.34	0.50
	15 (15)	0.242	0.43	0.67
	5 (8)	0.201	0.27	0.47
	1 (7)	-0.013	0.12	0.10
		0.136		

	cluster_id (size)	Average changes in pdx	T41	X41
Patient #13	7 (105)	0.335	0.17	0.50
	1 (14)	0.685	0.29	0.97
	6 (5)	0.045	0.11	0.16
		0.355		

	cluster_id (size)	Average changes in pdx	T58	X58
Patient #6	4 (129)	0.166	0.34	0.50
	2 (28)	0.456	0.53	0.99
	1 (5)	-0.009	0.14	0.13
		0.204		

		Average changes in pdx	T43	X43
Patient #16	3 (93)	0.101	0.40	0.51
	2 (9)	0.233	0.77	1.00
		0.167		

Supplementary Table S5. The ratio of truncal, branched and private mutations in each MOM case.

Patient	Truncal	Branched	Private	Total	Truncal (%)	Branched (%)	Private (%)
Patient #10	84	30	101	215	39.1%	14.0%	47.0%
Patient #14	48	19	95	162	29.6%	11.7%	58.6%
Patient #21	831	1,048	3,296	5,175	16.1%	20.3%	63.7%
Patient #34	72	50	71	193	37.3%	25.9%	36.8%
Patient #35	83	26	162	271	30.6%	9.6%	59.8%
				Average	30.5%	16.3%	53.2%
				Minimum	16.1%	9.6%	36.8%
				Maximum	39.1%	25.9%	63.7%

Supplementary Table S6. Summary of mutations in ERBB3, ERBB2, NF1 and PIK3CA genes from patient #21.

Gene	Genomic location	Amino acid change	Cosmic 70	X75 Primary	X74 Liver (8)	X79 Liver (3)	X80 Liver (6-2)	X91 Liver (6-1)	X81 Omentum	X82 Mesenteric	X191 Lymph node	X201 Liver (recur)	Drug
ERBB3	12:56481922	NM_001982:exon7:c.G850A:p.G284R	V	V	V	V	V	V	V	V	V	V	Lapatinib
ERBB2	17:37880220	NM_001289937:exon19:c.T2264C:p.L755S	V					V					
NF1	17:29552144	NM_000267:exon17:c.1877delT:p.L626fs		V	V	V	V	V	V	V	V	V	Trametinib
	17:29553478	NM_000267:exon18:c.2027delC:p.T676fs	V	V	V		V	V	V	V	V	V	
	17:29553485	NM_000267:exon18:c.2034delG:p.P678fs				V							
PIK3CA	3:178936092	NM_006218:exon10:c.A1634C:p.E545A	V				V						BYL719
	3:178937422	NM_006218:exon12:c.T1810C:p.C604R	V			V							
TP53	17:7576853	NM_000546:exon9:c.G993T:p.Q331H	V									V	
	17:7577121	NM_000546:exon8:c.C817T:p.R273C	V		V	V	V	V	V				
	17:7577547	NM_000546:exon7:c.G734A:p.G245D	V						V				
	17:7578454	NM_000546:exon5:c.C476T:p.A159V	V							V	V	V	